19th Brazilian Congress of Thermal Sciences and Engineering
November 06th-10th, 2022, Bento Gonçalves - RS - Brazil

ENC-2022-0121
MECHANISTIC MODELING OF THE SURGING PHENOMENON INITIATION IN CENTRIFUGAL PUMPS OPERATING WITH GAS-LIQUID TWO-PHASE FLOW

Cesar Alata
Henrique Stel
Rigoberto E.M. Morales
Multiphase Flow Research Center (NUEM), Federal University of Technology – Paraná (UTFPR). Rua Deputado Heitor Alencar Furtado 5000, Bloco N, CEP 81280-340, Curitiba, Brazil
cesarq@alunos.utfpr.edu.br
henrique.azevedo@funtefpr.org.br
rmorales@utfpr.edu.br

Abstract. *In the oil industry, one of the most used techniques for artificial lift consists of electric submersible pumps. The presence of gas in the reservoirs gives rise to liquid-gas flow, causing a drastic degradation of the pump's performance, a condition known as surging. This occurrence significantly affects the pump production and service life, as centrifugal pumps are designed to operate only with single-phase liquid flows. There are several studies in the literature on the phenomenon of surging, both experimental and numerical, providing valuable information for its understanding. However, attempts to obtain mechanistic models for its prediction have limitations for assessing the overall performance of the pump for different operating conditions, so their application is questionable. In this sense, the present study seeks to present a mechanistic model that better represents the dominant mechanisms of the surging phenomenon. An approach to predict the starting point of surging is proposed, to have a better assessment of the pump operating window without serious performance degradation. This could lead to more reliable decisions in the pump operation under gas-liquid flows, consequently improving the pump efficiency and applicability for such scenarios.*

Keywords: *two-phase, surging, centrifugal pumps, mechanistic model.*

1. Introduction

Two-phase flows generally involve complex physical phenomena that are difficult to understand. Given the chaotic nature of fluid behavior depending on several geometric, physical, and chemical parameters, obtaining models for the most adequate prediction of these flows that apply to practical scenarios is quite complex. However, the industry shows increasing interest in understanding the behavior of two-phase flows in various operational processes, an example being the case of pumping liquid-gas mixtures, which is common in sectors such as the nuclear industry and oil extraction.
Depending on the characteristics of the wells, the oil may contain a significant amount of gas, which will flow through the well in the form of a two-phase mixture. This mixture can cause significant degradation in the performance of Electric Submersible Pumps (ESP), reducing their lifting capacity and oil production and, consequently, causing economic losses. The effect caused by the suction of different volumetric fractions of gas, causing losses in pump performance, specifically in pump pressure rise, can be observed in performance through the characteristic curves shown in Figure 1.

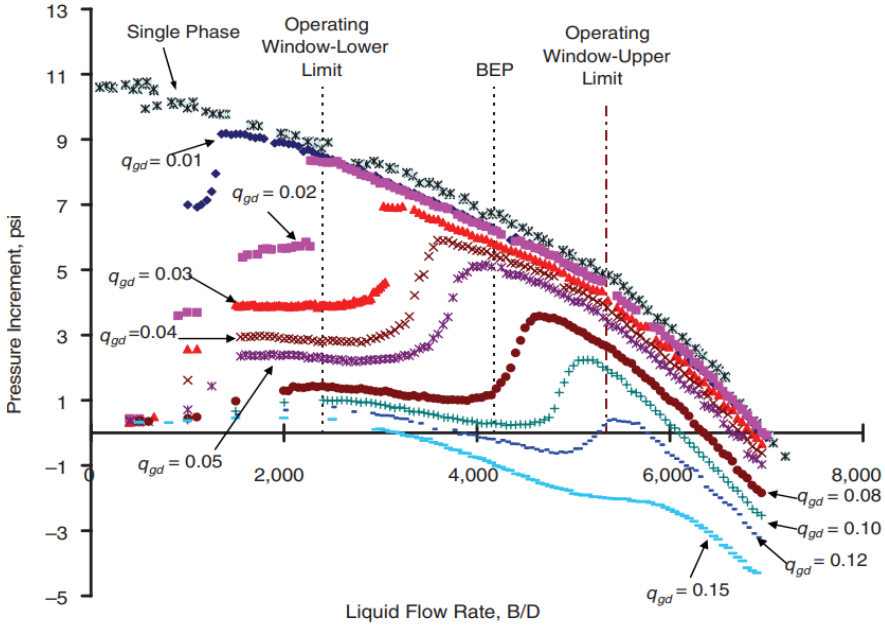

Figure 1. Performance curves of a centrifugal pump operating with two-phase and single-phase flow (Gamboa, 2008).

Figure 1 describes the behavior of pressure curves as a liquid flow ratio operating with various volumetric fractions of gas. In the case of single-phase pumping, the gas fraction is zero. As the amount of gas in the pump suction increases, the greater will be the degradation of its performance and, consequently, the pressure gain. This drop becomes more significant as the liquid flow decreases when a zone of unstable pump operation is reached, called "*surging*" (Lea and Bearden, 1982).
After the onset of *surging*, the gas can form pockets in the impeller channels, which in turn causes fluctuations in system pressure. At the same time, performance drops sharply, entering an unstable zone of operation until eventually completely blocking the rotor channel. The *surging* phenomenon, which corresponds to the pump's unstable performance zone under two-phase flow, is directly linked to its useful operating window. The identification of this window is of interest due to safety issues in the nuclear industry as well as production costs in the oil industry.

Most studies on the phenomenon of *surging* are experimental and few analytical studies are approaching the physics of the phenomenon. Table 1 provides a summary of the main studies on two-phase liquid-gas flow models in centrifugal pumps associated with *surging* phenomena. Among the mechanistic models for *surging* prediction, empirical correlations were developed from regressions of experimental data, which can hardly be extended to other ESP geometries. Currently, the existing models are heavily dependent on empirical data.

Among the *surging* models that are not entirely based on empirical correlations are the proposals by Barrios (2007) and Zhu et al. (2017), both of which employ a mechanistic approach to determine the *surging* onset. However, different criteria are used to determine this onset. For instance, although both the Barrios (2007) and the Zhu et al. (2017) models are based on the evaluation of a critical bubble diameter related to *surging*, the former takes this critical size as the limiting condition at which the bubbles will get stuck into the impeller channels, while the latter assumes that this critical condition will start significant bubble deformation. Such studies need to be validated with experimental data, so the extension of their applications for different pumps is questionable.

Stel (2019) developed an experimental and numerical study of liquid-gas flow in a centrifugal rotor. The author observed three types of patterns for different conditions, namely, dispersed bubbles, intermittent gas pockets after the *surging point*, and large gas pockets. From there, he proposed a mechanistic model for *surging* at low intake gas flow rates, in an attempt to make little use of calibration data. However, the model proved to be very sensitive to many parameters that are hard to estimate, such as the bubble diameter and the drag coefficient.

Table 1 - Summary of the main studies

Study	Authors	Contributions	Limitations
Models	**Turpin (1986)**	A correlation factor for *Surging*	Empirical model
	Cirilo (1998)	Correlates gas fractions and inlet pressure to *surging* conditions	Empirical model
	Barrios (2007)	Generates a mechanistic model for *surging* considering bubble diameter and drag coefficient	The model can not be extended to other pump types
	Gamboa (2008)	*Surging* model as a function of the suction gas volume fraction	Need experimental data
	Zhu et al. (2017)	*Surging* model as a function of the suction gas volume fraction	Need experimental data
	Stel (2019)	Mechanistic model, no need for empirical data	Works only for low intake gas flow rates, needs bubble diameter information

As one can see, more mechanistic models for *surging* based on the physics of the phenomenon are necessary, to better represent its initiation mechanisms and thus define a more realistic operational window under stable conditions, through a wide range of operating conditions.
In this work, we propose a mechanistic model to predict the *surging* onset. The model is an improvement of the Stel (2019) approach, where many assumptions and correlations assumed by the author were reassessed, supported by experimental and numerical data from literature.

2. Mechanistic modeling of the *Surging* initiation

The proposed model was based on the inability of a bubble to move inside the rotor. This criterion is the fundamental hypothesis adopted by Estevam (2002), Barrios (2007) and Stel (2019). A criterion based on physical grounds instead of purely empirical data has the advantage of avoiding excessive calibration parameters. However, several simplifications have to make the problem tractable.
One fundamental aspect of the model for predicting the starting point of *surging* resides in the existence of a delay in the gas velocity in relation to the liquid such that, at some point, the bubble will tend to stop in the rotor. The point where this stop will occur, however, is not very clear. For instance, Barrios (2007), based on experimental visualization, assumes that this should occur at the rotor inlet, while Stel (2019) considers that the rotor outlet is the most critical region since it is where one finds the maximum centrifugal force acting from the liquid on the bubbles. Independently on the exact position, it is assumed in all models that, if the bubbles are not able to leave the impeller, they will start a process of coalescence with other incoming bubbles, initiating the formation of pockets that, in turn, will induce the enormous hydraulic losses associated with the occurrence of *surging*.

Figure 2 schematically represents the movement of a bubble through the liquid inside the rotor. In (a) the trajectory of a bubble and streamlines of the liquid are shown, with an indication of the velocities of both the bubble and the liquid. In (b), the distributions of the main forces acting on the bubble are indicated, namely: force due to the pressure gradient, $\vec{F}_P$, drag force $\vec{F}_D$, resultant centrifugal force of the liquid on the bubble, $\vec{F}_{Centr,L\to b} = \forall_b \rho_L \vec{\Omega} x(\vec{\Omega} x\vec{r})$, where $\forall_b$ is the volume of the bubble; resultant *Coriolis* force of the liquid on the bubble, $\vec{F}_{Cor,L\to b} = -\forall_b \rho_L \vec{V} x\vec{\Omega}$, and the sum of the other interfacial forces (virtual mass, lift, etc.) of the liquid on the bubble, $\sum \vec{F}_{R,L\to b}$.

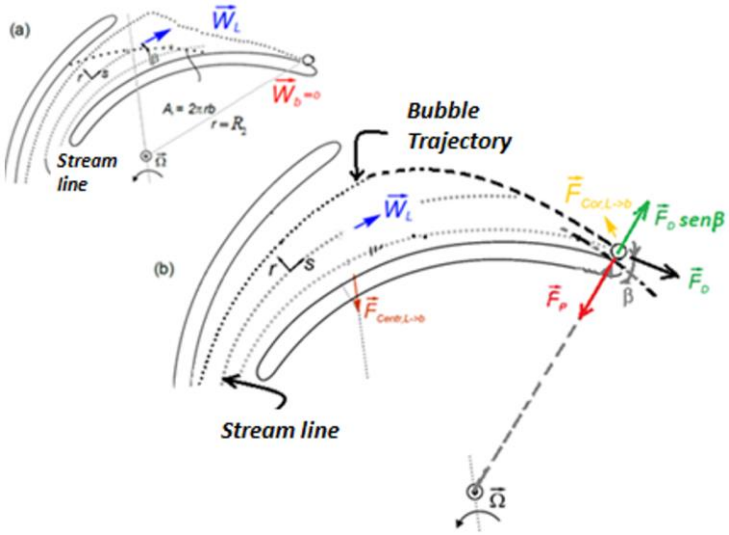

Figure 2. Illustration of the movement of a bubble along its trajectory: (a) representation of the bubble and liquid velocities, at an arbitrary point inside the rotor; (b) orientation of drag, pressure, Coriolis and centrifugal forces acting on the bubble.

To obtain the model, other hypotheses need to be taken to make the problem tractable. The velocity of the liquid phase in a radial position r can be approximated as the average liquid velocity calculated from the liquid flow rate, $V_L = Q_L / (A_r sen(\beta)) = Q_L / (2\pi rbsen(\beta))$, where A_r is a meridional area of the channel as a function of r, β is the blade angle at the same point and b is the channel height. Since the Coriolis force is almost always perpendicular to the bubble motion and the drag and pressure gradient forces are dominant, the term $\sum \vec{F}_{R,L\to b}$ is neglected. The model does not neglect this increase in area, but shear stresses due to the wall and other effects on the pressure gradient are negleceted. The bubbles are considered as spherical, but the effect of their deformation on the drag force is taken into account (differently from most of the previous models, including Stel [2019]). It is also assumed that the passage of the bubbles does not significantly affect the liquid field around them, nor the movement of neighboring bubbles. The physical properties of both the liquid and gas phases are constant. Finally, the development here presented is developed for the particular case of radial rotors (although it could be slightly modified in the future to include mixed type impellers as well).

From the above conditions, it is reasonable to assume, as previously suggested by Murakami and Minemura (1974), and Barrios (2007), that a bubble flowing along with the along the "s" direction (that is, a direction which is aligned with the liquid streamlines) will be subject to an approximate equilibrium $\vec{F}_P$ and $\vec{F}_D \cos(\theta)$, such that:

$$\left|\vec{F}_P\right| = \left|\vec{F}_D \cdot cos(\theta)\right| \Rightarrow \frac{\pi d_b^3}{6}\frac{dp}{dr} = \left[\frac{1}{2}C_D\rho_L\frac{\pi d_b^2}{4}\left(w_L - w_b\right)^2\right]cos(\theta) \tag{1}$$

Above, C_D is the drag coefficient, and is the one-dimensional pressure gradient along the radial direction aligned to the "r". Being $\cos\theta$ angle that forms bubble trajectory and liquid streamline. The term $(dp/ds) \approx (dp/dr)$ can be approximated at the exit of the rotor blade, according to Barrios (2007), by hypothesis, as a component of the centrifugal force per unit volume of the liquid over the gas, $\vec{F}_{Centr,L\to b}$, decomposed on the coordinate "r", that is, $|\vec{F}_{Cor,L\to b}| \approx (dp/dr) = \frac{\rho_L}{r}\left[\left(\frac{Q_L}{2\pi rb}\right)^2 + \left(2\pi r\Omega\right)^2\right]$, where: Ω, ρ_L, Q_L the rotor angular velocity, liquid density, and liquid flow rate, respectively. Substituting this approximation in Eq. (1):

$$\left(w_L - w_b\right) = \sqrt{\frac{4d_b}{3C_D}\left(\frac{\rho_L}{r}\left[\left(\frac{Q_L}{2\pi rb}\right)^2 + \left(2\pi r\Omega\right)^2\right]\right)\left(\frac{1}{\rho_L}\right)\left(\frac{1}{cos(\theta)}\right)} \tag{2}$$

Based on Estevam (2002) and Barrios (2007), the main hypothesis of the model assumes, then, that in the limit condition of *surging*, the bubble will tend to stop at the rotor. Therefore, its net movement through "s" will be null, such that $v_b \to 0$. Unlike Barrios (2007) or Stel (2019), however, the model will be obtained as a function of the radial position

r where the surging occur, so that the sensitivity of the solution to this parameter can be investigated. Substituting $w_b = 0$ in (2), it is possible to estimate the liquid flow, $Q_L|_{surging}$, over which, under the assumed conditions, the probable point of *surging* on the performance curve should occur:

$$Q_L|_{surging} = 8(\pi r)^2 b\Omega\sqrt{\frac{d_b \cdot cos(\theta)}{3rC_D - 4d_b \cdot cos(\theta)}} \tag{3}$$

As the bubbles are assumed to be non-spherical, deformable and the system is slightly contaminated and the influence of neighboring bubbles on each other is neglected, the Tomiyama's model (Tomiyama et al., 1998) for the drag coefficient C_D is considered. The original model is given by Eq. (4), which is a function of the Reynolds number of the particle, (Re_P) and the Eötvos number. Following Ofuchi et al. (2022), however, it is convenient to use a different acceleration scale when calculating the Eötvos number, since the original definition for this variable is based on the gravitational acceleration as the main mechanism creating a tendency to deform the bubbles, while in the present case the centrifugal acceleration is the dominant one. This modified Eötvos number is referenced as EoC, which is calculated as in Eq. (5).

$$C_D = max\left\{min\left(\frac{72}{Re_p}; \frac{24}{Re_p}\left(1+0.15Re_p^{\,0,687}\right)\right); \frac{8}{3}\frac{EoC}{EoC+4}\right\} \tag{4}$$

$$EoC = Eo \cdot G = \frac{(\rho_L - \rho_G)\Omega^2 r D_B}{\sigma} \tag{5}$$

$$Re_P = w_L.d_b.\rho_L / \mu_L \tag{6}$$

Note that Re_P depends on the liquid velocity (w_L), which is linked to the liquid flow we want to find in Eq. (3). An iterative solution is thus necessary, but one that tends to quickly converge to a reasonable initial estimate for liquid velocity (w_L).

Furthermore, the model depends on the specification of the bubble diameter subjected to *surging*, d_b. Stel (2019) observed that, for a range of rotating speeds from 200 to 500 rpm, maximum bubbles found inside the rotor in his study were between 3 e 4 mm. However, pumps normally work at moderate to high rotation speeds, such that the range of diameters in which the bubble actually enter the impeller tends to be restricted due to breakage phenomena. For this purpose, a reasonable approach is to identify, as a critical situation, the maximum possible diameter with which the gaseous phase can enter the rotor, as a function of the operating conditions. The geometry and specification of the main rotor dimensions studied by Stel (2019) is shown in Fig. 3, which he used to compare results with his model.

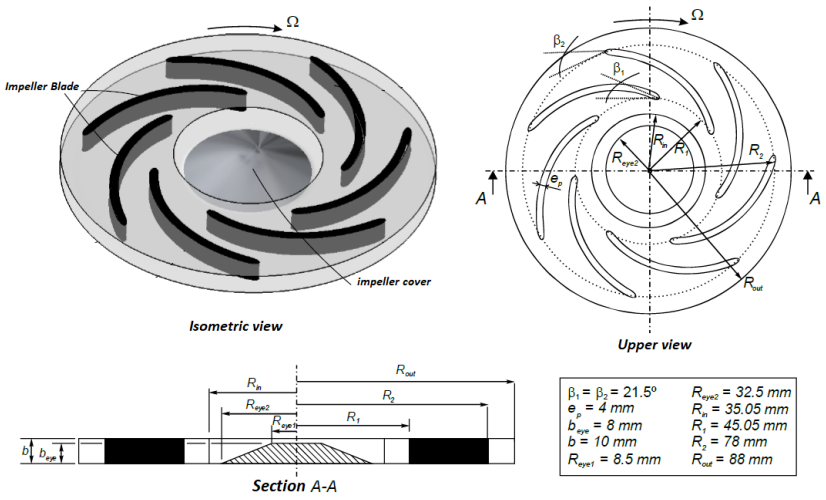

Figure 3. Views and species specifications of the main dimensions (isometric, top, and side) of the centrifugal rotor assumed in the study.

A bubble entering a centrifugal rotor is normally subject to the transition from a region of favorable pressure gradient (such as a tube or diffuser) to a rapid deceleration in the rotor channel, where the pressure gradient suddenly becomes unfavorable to its motion. Kolev (2002) argues that a criterion to assess the stability of bubbles and drops, under these conditions, can be obtained by evaluating the Weber number (We), calculated as a function of the difference in velocity between the phases:

$$We = \frac{\rho_L (w_L - w_b)^2}{\sigma / d_b} \tag{7}$$

The dimensionless number above derives from a balance between the drag force that acts to deform the bubble and the surface tension σ, which acts to keep it stable.

Through a scale analysis for spherical bubbles, Kolev (2002) suggests that the critical Weber number (We), for which a bubble or drop can withstand a break, has an upper limit $We \approx 20$. This limit must be much lower, in practice, for high Reynolds numbers, and even lower for cases where the bubble is suddenly subjected to a difference in velocity. The author proposes a correlation for a critical Weber number, We_C, in the latter case, as a function of the Reynolds number of the particle and the Ohnesorge number (On), $On = We^{1/2} / Re_P$.

$$We_c = 55\left(\frac{24}{Re_P} + \frac{20{,}1807}{Re_P^{0{,}615}} - \frac{16}{Re_P^{2/3}}\right)(1 + 1{,}077 On^{1{,}64}), 200 < Re_P < 2000 \tag{8}$$

$$We_c = 55(1 + 1{,}077 On^{1{,}64}), Re_P \geq 2000 \tag{9}$$

Se $Re_P < 2000$, $On > 4$ ou $We < We_C$, The bubble is stable and does not fragment.

To evaluate the critical diameter of bubbles at the impeller inlet, $d_{b,c}$, Eq. (2) is solved using $r = R_1$ and $\beta = \beta_1$ replacing the expression obtained for $(w_L - w_b)$ in Eq. (5). Then Eqs. (5) to (7) are to solved for $d_b = d_{b,c}$ to find a critical breakage condition. An iterative solution is necessary, because the resulting expression cannot be solved analytically, since C_D, Re_P and On are functions of $d_{b,c}$ and $(w_L - w_b)$. However, the solution quickly converges with reasonable initial estimates for these last two quantities.

For the geometric parameters of the rotor assumed in this work, the critical inlet diameter for the geometric parameters of the rotor assumed in this work, the critical inlet diameter, $d_{b,c}$, as a function of the rotational speed, n, was solved. The result is shown in Figure 4. Note that $d_{b,c}$ drops rapidly with n, being approximately 7 mm for 200 rpm, 4.9 mm for 300 rpm, and 3 mm for 500 rpm, reducing to 0.6 mm for 3500 rpm. In particular, the range found for 300 to 500 rpm agrees relatively well with the maximum bubble diameters experimentally measured by Stel (2019), observed as never larger than 4.0 mm in the impeller.

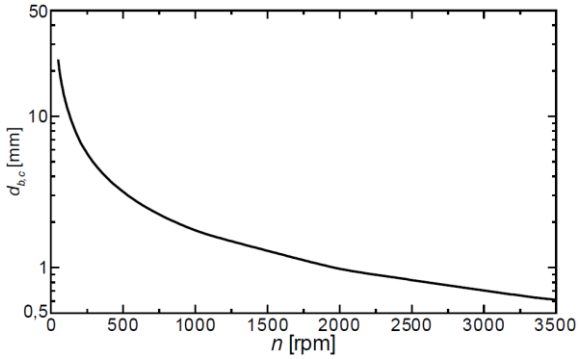

Figure 4. Variation of critical bubble diameter at impeller inlet with rotational speed (Stel, 2019).

Figure 4 refers to the maximum possible diameter, and in practice, the maximum value actually found inside the rotor may be smaller due to the gas injection method used. Note, for example, that at extremely low rotational speeds, very large bubbles (above 20 mm) are possible by the above criterion, but that in practice they do not occur in dispersed bubble patterns. Furthermore, very low rotational speeds are not of interest for the vast majority of centrifugal pump operations. Still, in commercial pump rotors, the breakage can be even greater due to the close proximity of the leading edge of the

rotor eye blades, which tends to generate high levels of turbulence. Thus, the above criterion can be used, in the absence of any other information regarding the way in which the gas enters the rotor, as a conservative estimate.

It should be mentioned that Stel (2019) used an aerator that generated bubbles generally smaller than 4.0 mm at the rotor inlet for the lowest gas flows rates. This value was used together with the criterion for the critical diameter, as a way of approaching the maximum diameter of bubbles that enter the rotor, to calculate the *surging* indicator boundary.

2.1 Pressure gradient in the impeller channel

The centrifugal rotor produces an increase in the pressure of the liquid, from the entrance to the exit of the channel. This pressure gradient creates a buoyancy force, generally referred to as the pressure gradient force (Murakami and Minemura , 1974) that acts from the liquid on the bubbles, tending to push them back to the rotor inlet. Providing a good estimation for this force is critical to the performance of the model.
Figure 5 shows a comparison for estimations of the pressure gradient along the path of the rotor channel, using different methodologies, namely: the Murakami and Minemura (1974) model; the Barrios (2007) model; the combined numerical/experimental data from Ofuchi et al. (2022).
The Murakami and Minemura (1974) model (which was also used by Stel, 2019) assumes a simplified model for the pressure gradient, where it is approximated as a component of the centrifugal force acting along an idealized trajectory of the bubble, $\frac{dp}{ds} \approx \rho_L \omega^2 r \cdot sen(\beta)$. In turn, the pressure gradient expression proposed by Barrios (2007) is also based on an the centrifugal acceleration. However, it was taken as acting in the radial direction, without being decomposed on the direction of the bubble idealized trajectory. It also considers the additional increase in pressure associated to the area increase of the rotor channel in the radial direction. The resulting expression used by Barrios (2007) is $\frac{dp}{dr} = \frac{\rho_L}{r}\left[\left(\frac{Q_L}{2\pi r b}\right)^2 + (2\pi r \Omega)^2\right]$.

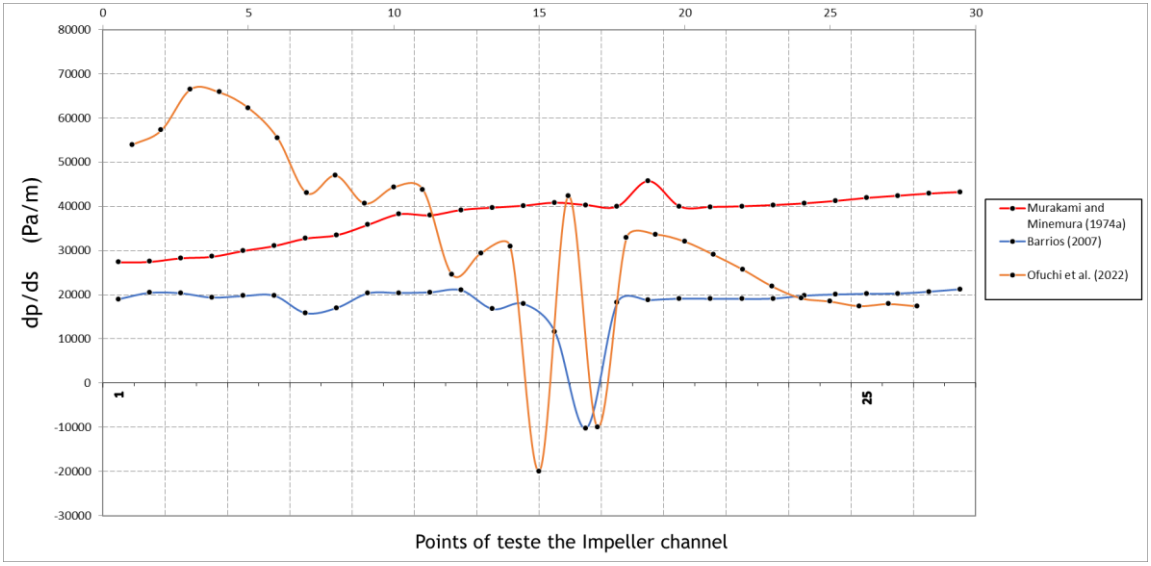

Figure 5 - Pressure gradient comparison along the centrifugal rotor channel.

The pressure gradient estimated by Ofuchi et al. (2022) for a real bubble trajectory reveals a highly oscillating trajectory as the bubble advances through the rotor, because of turbulence, rapid changes in bubble direction, bubble deformation, effect of non-drag forces, etc. Estimating this behavior with simple, analytical models seems like an impractical task. Also, at any point along the bubble trajectory, the Murakami and Minemura (1974) model agrees poorly with the Ofuchi et al. (2022) data.
On the other hand, the pressure gradient model proposed by Barrios (2007) at the exit of the channel blade is found to give results in the same order of magnitude as the experimental data. This model was thus used in the present study.

3. Results

Figure 6 shows the surging boundary curves obtained with the proposed model at different radial positions, compared with the experimental results from Stel (2019) for an inlet gas flow rate of $\dot{m}_G = 0,06$ kg/h. Although the model is used to obtain only the liquid flow rate associated to the surging initiation, the surging boundary curve shown in the figures was obtained by estimating the correspondent ΔP value in the single-phase flow curve.
In general, one can observe that the model is highly sensitive to the actual point at which the bubble stops in the rotor channel. Figure 6 (a) shows that, for $r = R_2/4$, the model overestimates the liquid flow rate associated to surging, given results far from the experimental values. In turn, Figs. 6 (c), and (d) show that, for $r = R_2/12$ and $R_2/16$, the model underestimates the surging initiation. Results with $r = R_2/8$, however, agree well with the experimental data, as one can observe in Fig. 6 (b).

Figure 6 (a). Figure 6 (b).

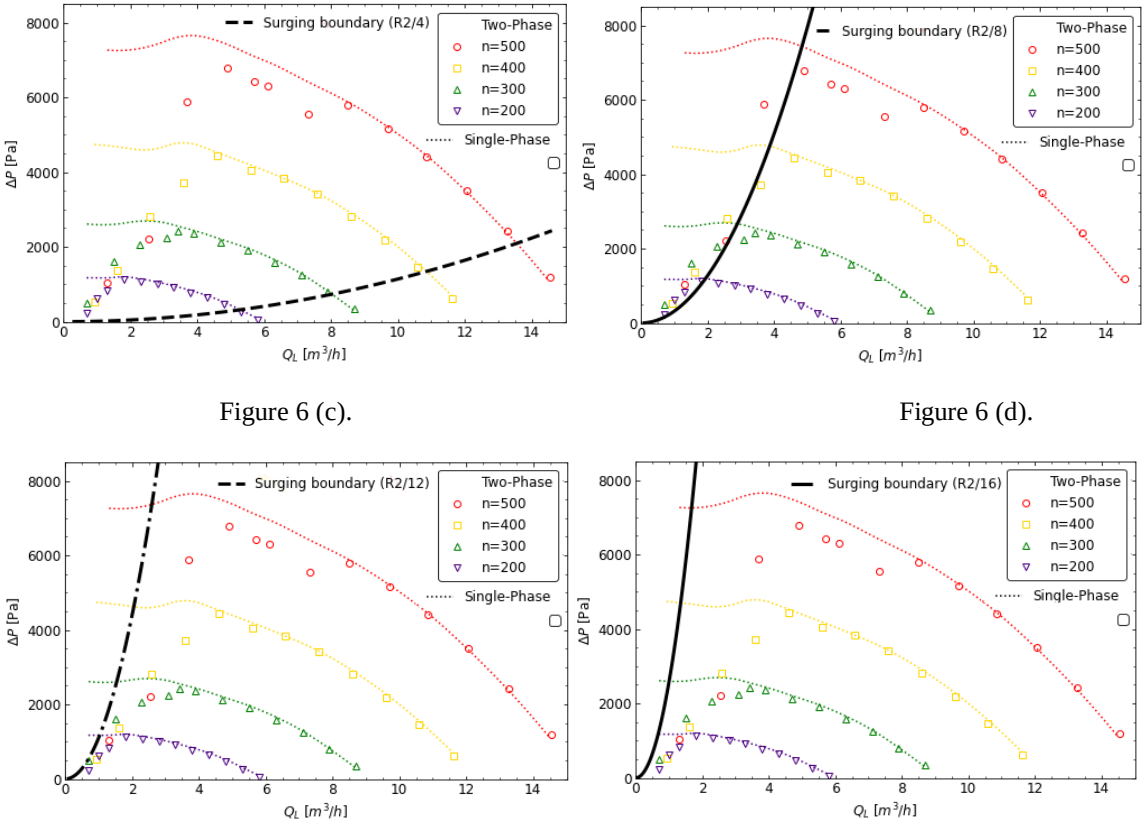

Figure 6 (c). Figure 6 (d).

Figure 6 - Indication of *surging* boundary for different radius, (a) $r = R_2/4$, (b) $r = R_2/8$, (c) $r = R_2/12$, and (d) $r = R_2/16$, together with experimental curves (Stel, 2019) of rotor pressure gain obtained for single-phase and two-phase flow ($\dot{m}_G = 0,06$ kg/h)

The *surging* boundary obtained with the proposed model using $r = R_2/8$ is shown in Fig. 7 together with results obtained with other models from literature, namely the ones from Duran (2003), Gamboa and Prado (2011) and Zhu et al. (2017). One can see that the proposed model gives results relatively close to the surging boundary measured experimentally, while the other models significantly underestimate the surging initiation. This difference can be attributed to the many empirical components contained in the other models, which certainly perform well when compared with the experimental values at which they were calibrated for, but eventually cannot be extended for other scenarios. Mechanistic models, on the other hand, tend to be much less sensitive to calibration parameters.

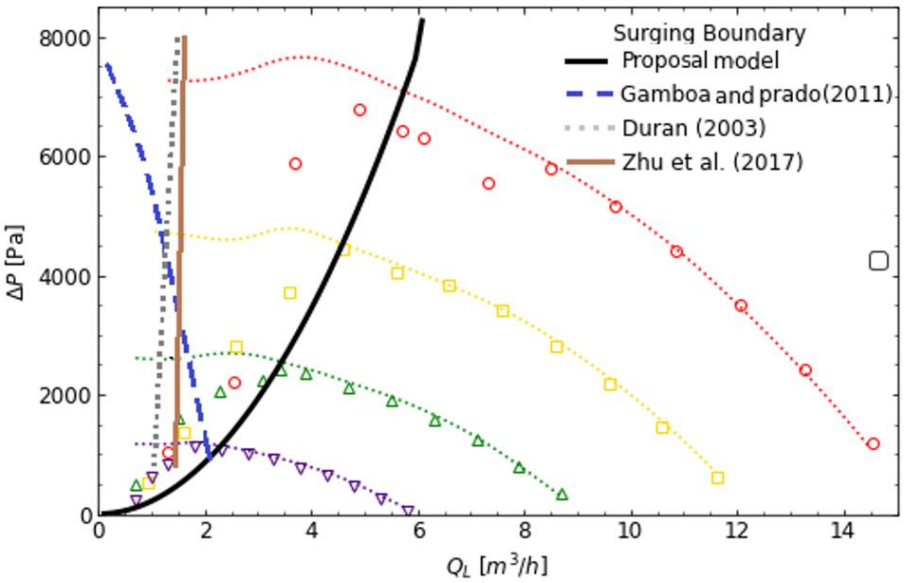

Figure 7. Comparison of the *surging* boundaries obtained with the proposed methodology with other models in the literature, shown over rotor experimental pressure gain curves (Stel, 2019) under single-phase and two-phase flow at low inlet gas flow rate ($\dot{m}_G = 0,06$ kg/h).

4. Conclusions

This work concerns the development of a mechanistic model for the onset of surging in centrifugal pumps. The model is based on the calculation of a velocity delay between a bubble moving through the rotor channel and the surrounding liquid, which depends on estimations for the drag and pressure gradient forces acting on the bubble. Results for the liquid flow rate associated to surging were compared with experimental data.

The model improves the methodology from Stel (2019), especially by using the Barrios (2007) model for the pressure gradient over the bubble, since it better represents the pressure gradient acting on bubbles in a rotor channel, and consequently improves the results.

One important parameter considered in the model is the drag coefficient. Following Ofuchi et al. (2022), a model was used to include not only inertial and viscous force effects, but also the effects of surface tension and centrifugal acceleration on the bubble deformation.

The model is also found to be quite sensitive to the radius where surging will take place, that is, the point where the bubble will actually stop into the rotor, starting the coalescence with other incoming bubbles that will rapidly generate gas pockets. Results with the present model suggests that this should occur closer to the rotor inlet than near the outlet, which agrees with the assumption taken in the model from Barrios (2007). It is expected that this model, being much less dependent on empirical data than many models from literature, could be extended for different pump geometries and operating conditions, helping engineers to identify a safe operational window of centrifugal rotors operating with gas-liquid flows.

5. Acknowledgements

The authors are thankful to the NUEM/CENPES/PETROBRAS for the financial and technical support for this study.

6. References

Barrios, L. “Visualization and Modeling of Multiphase Performance inside an Electrical Submersible Pump”. 267 f. Ph.D. Thesis, The University of Tulsa. Tulsa, 2007.

Estevam, V. “A Phenomenological Analysis of Centrifugal Pump Operation with Two-Phase Flow. 297 p. Ph.D. Thesis (in Portuguese), Campinas State Univesity. Campinas, 2002.

Gamboa, J. “Prediction of the Transition in Two-Phase Performance of an Electrical Submersible Pump”. 286 f. Ph.D. Thesis (in Portuguese), The University of Tulsa. Tulsa, 2008.

Murakami, M.; Minemura, K. Effects of Entrained Air on the Performance of a Centrifugal Pump (First Report, Performance and Flow Conditions). Bulletin of the JSME, p. 1047-1055, 1974.

Ofuchi, E. M.; Silva, H. L. V.; Bertoldi, D.; Mancilla, E.; Stel, H.; Morales, R. E. M. Study of the bubble motion in a centrifugal rotor based on visualization in a rotating frame of reference. Chemical Engineering Science, v. 259, p. 117829, 2022.

Stel, H. “Numerical and Experimental Study of the Two-Phase Liquid-Gas Flow in a Centrifugal Rotor” 214 p. Ph.D. Thesis (in Portuguese), Federal University of Technology. Curitiba, 2019.

Tomiyama, A.; Kataoka, I.; Zun, I.; Sakaguchi, T. Drag coefficients of single bubbles under normal and micro gravity conditions. JSME International Journal Series B, v. 41, n. 2, p. 472-479, 1998.

Zhu, J.; Guo, X.; Liang, F.; Zhang, H. “Experimental Study and Mechanistic Modeling of Pressure Surging in Electrical Submersible Pump”. Journal of Natural Gas Science and Engineering, v. 45, p. 625-636, 2017.

Lea, J. F.; Bearden, J. L. Effects of Gaseous Fluids on Submersible Pump Performance. Journal of Petroleum Technology, v. 24, p. 2922-2930, 1982

Zhu, J.; Guo, X.; Liang, F.; Zhang, H. Experimental Study and Mechanistic Modeling of Pressure Surging in Electrical Submersible Pump. Journal of Natural Gas Science and Engineering, v. 45, p. 625-636, 2017.

Turpin, J. L.; Lea, J. F.; Bearden, J. L. Gas-Liquid through Centrifugal Pumps Correlation of Data. In Proceeding of the Third International Pump Symposium, 1986, College Station. p. 13-20

Cirilo, R. Air-Water Flow Through Electrical Submersible Pumps. 81 f. Dissertation (Master), The University of Tulsa. Tulsa, 1998.

Kelev, N. I. Multiphase Flow Dynamics 2. 2 a Ed. New York: Springer, 2002.

Duran, J. Pressure Effects on ESP Stages Air-Water Performance. 171 f. Dissertation (Master), The University of Tulsa. Tulsa, 2003

7. The author(s) is (are) the only responsible for the printed material